

Parsimonious Optimisation of Parameters in Variational Quantum Circuits

Sayantana Pramanik^{1,2}, Chaitanya Murti¹, and M Girish Chandra³

¹Robert Bosch Centre for Cyber-Physical Systems, Indian Institute of Science

²Corporate Incubation, TATA Consultancy Services, Bengaluru, India

³TCS Research, TATA Consultancy Services, Bengaluru, India

Variational quantum circuits characterise the state of a quantum system through the use of parameters that are optimised using classical optimisation procedures that typically rely on gradient information. The circuit-execution complexity of estimating the gradient of expectation values grows linearly with the number of parameters in the circuit, thereby rendering such methods prohibitively expensive. In this paper, we address this problem by proposing a novel Quantum-Gradient Sampling algorithm that requires the execution of at most two circuits per iteration to update the optimisable parameters, and with a reduced number of shots. Furthermore, our proposed method achieves similar asymptotic convergence rates to classical gradient descent, and empirically outperforms gradient descent, randomised coordinate descent, and SPSA.

1 Introduction

The quantum processors available today are limited in terms of the number of qubits available, their coherence times, noise-resilience, etc. This phase has been dubbed as the Noisy, Intermediate-Scale Quantum era [1]. Variational Quantum Algorithms (VQAs) [2, 3, 4, 5, 6] - which employ both quantum and classical processors to work in tandem - investigate and utilise their potential for solving various problems in Chemistry, Machine Learning and Optimisation. In VQAs, we operate under the premise that a variational circuit represented by $U(\boldsymbol{\theta})$ acts on the conventional initial state $|0\rangle^{\otimes n}$ of the qubits, to obtain the state $|\psi(\boldsymbol{\theta})\rangle = U(\boldsymbol{\theta})|0\rangle^{\otimes n}$; for the sake of brevity, the superscript $\otimes n$ will henceforth be dropped. We assume the circuits consist of single-qubit Pauli rotation gates, along with 2-qubit CX s, which together form a universal set of quantum logic gates. The rotational gates are parameterised by the list of parameters $\boldsymbol{\theta} \in \mathbb{R}^k$. The objective of variational algorithms is to find $\boldsymbol{\theta}^*$ such that:

$$\boldsymbol{\theta}^* = \arg \min_{\boldsymbol{\theta}} \langle \psi(\boldsymbol{\theta}) | H | \psi(\boldsymbol{\theta}) \rangle \quad (1)$$

for a Hermitian observable H . To simplify notation, we use:

$$\mu_{\boldsymbol{\theta}} = \langle \psi(\boldsymbol{\theta}) | H | \psi(\boldsymbol{\theta}) \rangle \quad (2)$$

Sayantana Pramanik: sayantana@iisc.ac.in

Chaitanya Murti: mchaitanya@iisc.ac.in

M Girish Chandra: m.gchandra@tcs.com

The current state-of-the-art method for estimating quantum gradients of expectation values for use in first-order methods for variational quantum algorithms is the parameter-shift rule (PSR) [7, 8]. PSR is equivalent to the finite-difference method, except that individual parameters are perturbed by finite values s_i , thus giving us a formula for gradients of single-qubit Pauli rotations as:

$$\frac{\partial \mu_{\theta_i}}{\partial \theta_i} = \frac{\mu_{\theta_i + s_i} - \mu_{\theta_i - s_i}}{2} \quad (3)$$

where $s_i = \pi/2$. However, PSR requires running the quantum circuits (for a certain number of shots) twice, with $\theta_i + s_i$ and $\theta_i - s_i$, respectively to obtain the gradients with respect to each individual parameter. Thus, the total number of circuits evaluated is $2k$ at each iteration of the optimization routine, which prohibits scalability.

Several recent works have acknowledged the importance of reducing the number of quantum measurements, and have developed techniques for shot-frugal optimisation [9, 10, 11, 12]. However, the number of measurements is calculated as the product of circuits executed and the shots they were run for. This is relevant because many cloud-providers that provision access to gate-model quantum processors employ separate pricing strategies for each circuit that is executed, and the number of shots it is executed for. Table 1 provides an overview of the cost incurred in running each circuit and each shot on various quantum processors. Evidently, the per-circuit price appears to be 10-1000 times more expensive than per-shot price.

Processor	Per-circuit price (USD)	Per-shot price (USD)
IonQ - Harmony	0.3	0.01
IonQ - Aria	0.3	0.03
OQC - Lucy	0.3	0.00035
Rigetti - Aspen-M	0.3	0.00035

Table 1: Per-circuit and per-shot prices for running circuits on real gate-based quantum processors through a popular cloud service provider.

As such, we feel that the field of minimising the number of circuit-executions is under-explored, with only a few methods proposed, the most widely used and studied of which is the classical technique of Simultaneous Perturbation Stochastic Approximation (SPSA) [6, 13, 14, 15]. SPSA also promises two circuit-evaluations for parameter-updation per iteration with perturbed parameters, and uses them to estimate the slope in the random direction [9]. However, it has been reported to be sensitive to the choice of hyperparameters [9], and as shown later in Sec. 4.1, not found to perform well for Quantum Machine Learning (QML) tasks. Besides gradient descent (based on PSR), and SPSA, the results from QGSA have also been compared against randomised coordinate descent [16], which randomly picks a parameter and updates it based on the gradient-estimate with respect to that parameter, resulting in two circuit runs. But it has been observed from the results in Sec. 4.1 that both SPSA and RCD end up consuming more iterations to converge.

To address these issues, we introduce the Quantum-Gradient Sampling Algorithm (QGSA) which requires at most two circuits to be executed (with a reduced number of shots) to update the parameters at each iteration. Furthermore, we show that it has the same asymptotic rate of convergence as gradient descent (GD). In practice, it was found to perform better than the aforesaid methods at a fraction of the number of measurements, as demonstrated in Sec. 4.1.

2 The Quantum Gradient Sampling Algorithm

In this section, we state Algorithm 1, our proposed Quantum-Gradient Sampling Algorithm. The algorithm uses only two circuit evaluations to update the parameters in the variational quantum circuit, in contrast to the $2k$ evaluations necessitated by methods that estimate the gradients. It does this by utilising Theorem 3 and sampling random vectors from a bounded probability distribution.

We begin by stating the following assumption.

Assumption 1. *Going forward, without any loss of generality, we assume that the eigenvalues of the Hermitian observable H lie in $[0, 1]$.*

We note that H may be expressed as a linear combination of Pauli operators P_i with real coefficients c_i :

$$H = \sum_i c_i P_i \quad (4)$$

The observable H may be normalised as follows to obtain another Hermitian observable H' whose eigenvalues lie in the range $[0, 1]$ ¹:

$$H' = \frac{1}{2} \left(\frac{H}{\sum_i c_i} + I \right) \quad (5)$$

Our algorithm differs from classical gradient descent algorithms since instead of estimating the gradient, a random vector that is sufficiently close to the gradient is used as a descent direction. This yields an iterative algorithm, where the parameters $\boldsymbol{\theta}^{(t)}$ at the t^{th} iteration are updated as:

$$\boldsymbol{\theta}^{(t+1)} = \arg \min(\mu_{\boldsymbol{\theta}^{(t)} - \alpha_t \mathbf{g}_s}, \mu_{\boldsymbol{\theta}^{(t)} + \alpha_t \mathbf{g}_s}) \quad (6)$$

where $\alpha_t > 0$ is the step-size, $\mathbf{g}_s \in \mathbb{R}^k$ is a random vector whose components are i.i.d and sampled from a bounded probability distribution, as per Theorem 3, (for instance, $Uniform(-2\sqrt{\mu_{\boldsymbol{\theta}}}, 2\sqrt{\mu_{\boldsymbol{\theta}}})$). QGSA relies on the fact that the bounds on the distribution decrease as the value of the objective function decreases at each iteration. The update rule 6 can be written as

$$\boldsymbol{\theta}^{(t+1)} = \boldsymbol{\theta}^{(t)} - s_t \alpha_t \mathbf{g}_s \quad (7)$$

with $s_t = -\text{sgn}(\mathbf{g}_t^\top \mathbf{g}_s)$, and \mathbf{g}_t being the actual gradient of $\mu_{\boldsymbol{\theta}^{(t)}}$. The update step executes only two circuits (with a reduced number of shots, as explained later in Sec 2.2.1), compared to $2k$ circuit executions required by methods that estimate the gradient using the parameter-shift rule [7]. We now state the Quantum-Gradient Sampling Algorithm formally in Algorithm 1.

We also provide another variant of the algorithm for use in the common setting wherein access to the gradient $\mathbf{g}_{\boldsymbol{\theta}}$ is unavailable. This algorithm is stated formally in Algorithm 2 in Appendix A.

¹S.P. would like to thank Dr. Sourav Chatterjee and Dr. Anirban Mukherjee, from the Corporate Incubation team at Tata Consultancy services, for helpful discussions regarding Hamiltonian normalisation.

Algorithm 1 Quantum-Gradient Sampling Algorithm

Inputs: initial point $\theta^{(0)}$, n_μ , n_g , ϵ

start

$\theta \leftarrow \theta^{(0)}$

do

evaluate μ_θ with n_μ shots

$\mathbf{g}_s \sim \mathbb{P}(-2\sqrt{\mu_\theta}, 2\sqrt{\mu_\theta})$ \triangleright where \mathbb{P} is a probability density function bounded between $-2\sqrt{\mu_\theta}$ and $2\sqrt{\mu_\theta}$

$\alpha \leftarrow \frac{|\mathbf{g}_\theta^\top \mathbf{g}_s|}{L \|\mathbf{g}_s\|_2^2}$ \triangleright where \mathbf{g}_θ is the gradient, and L is the Lipschitz smoothness constant of μ_θ

$\theta^- \leftarrow \theta - \alpha \mathbf{g}_s$

$\theta^+ \leftarrow \theta + \alpha \mathbf{g}_s$

evaluate μ_{θ^-} and μ_{θ^+} with n_g shots

$\theta = \arg \min(\mu_{\theta^-}, \mu_{\theta^+})$

while ($\|\mathbf{g}_\theta\|_2 \geq \epsilon$)

return θ

end

2.1 Perturbation bounds for quantum gradients

In this section, motivated by the need to use randomly sampled surrogates for gradients, we derive bounds on the gradients of expectation values in the quantum setting.

Before introducing bounds on the gradients of expectation values, we present the following helpful result:

Lemma 2. *If the i^{th} parameter θ_i of an ansatz $U(\theta)$, $i \in [k]$, is perturbed by a small quantity δ_i , such that the corresponding state changes from $|\psi\rangle_{\theta_i}$ to $|\tilde{\psi}\rangle_{\theta_i+\delta_i}$, then $\lim_{\delta_i \rightarrow 0} \|\psi\rangle_{\theta_i} - |\tilde{\psi}\rangle_{\theta_i+\delta_i}\| = |\delta_i|$, where $\|\cdot\|$ is the l_2 norm of a vector.*

Proof. We first define $|v\rangle$ such that $|\psi\rangle = U_{i+1:k}(\theta_{i+1:k})U_i(\theta_i)|v\rangle$, $|\epsilon\rangle = |\tilde{\psi} - \psi\rangle$, and note that $U_i(\theta_i) = e^{-i\theta_i G_i}$. Then,

$$\begin{aligned}
 \lim_{\delta_i \rightarrow 0} \langle \epsilon | \epsilon \rangle &= \lim_{\delta_i \rightarrow 0} \left(\langle \tilde{\psi} | \tilde{\psi} \rangle + \langle \psi | \psi \rangle - \langle \tilde{\psi} | \psi \rangle - \langle \psi | \tilde{\psi} \rangle \right) \\
 &= \lim_{\delta_i \rightarrow 0} \left(2 - \langle v | U_i^\dagger(\theta_i + \delta_i) U_i(\theta_i) | v \rangle - \langle v | U_i^\dagger(\theta_i) U_i(\theta_i + \delta_i) | v \rangle \right) \\
 &= \lim_{\delta_i \rightarrow 0} \left(2 - \langle v | (e^{-i\delta_i G_i} + e^{i\delta_i G_i}) | v \rangle \right) \\
 &= \lim_{\delta_i \rightarrow 0} (2 - \langle v | (2I \cos \delta_i) | v \rangle) \quad \text{since for } G^2 = I, e^{i\phi G} = I \cos \phi + iG \sin \phi \\
 &= \lim_{\delta_i \rightarrow 0} 4 \sin^2 \frac{\delta_i}{2} = \delta_i^2
 \end{aligned} \tag{8}$$

□

That is, if one of the parameters of a variational quantum circuit is perturbed by δ_i , then the magnitude of change in the corresponding state of the circuit is equal to the absolute value of the perturbation. In Theorem 3, we use this observation to derive non-trivial bounds on the derivative of μ_θ .

Theorem 3. *The partial derivative of $\mu_{\boldsymbol{\theta}}$ (as defined in Eq. (2)) with respect to θ_i lies in the range $[-2\sqrt{\mu_{\boldsymbol{\theta}}}, 2\sqrt{\mu_{\boldsymbol{\theta}}}]$, for all $i \in [k]$.*

Proof. Continuing with the notation in lemma 2, we have:

$$\langle \tilde{\psi} | H | \tilde{\psi} \rangle = \langle \psi | H | \psi \rangle + \langle \epsilon | H | \psi \rangle + \langle \psi | H | \epsilon \rangle + \langle \epsilon | H | \epsilon \rangle, \quad (9)$$

where the last term is of the order of δ_i^2 , and may be ignored, resulting in

$$\mu_{\theta_i + \delta_i} - \mu_{\theta_i} = \langle \epsilon | H | \psi \rangle + \langle \psi | H | \epsilon \rangle \quad (10)$$

Applying Cauchy-Schwarz inequality and noting that $\langle \psi | H^2 | \psi \rangle \leq \langle \psi | H | \psi \rangle$, we obtain:

$$-2\sqrt{\mu_{\boldsymbol{\theta}}} \|\epsilon\| \leq \mu_{\theta_i + \delta_i} - \mu_{\theta_i} \leq 2\sqrt{\mu_{\boldsymbol{\theta}}} \|\epsilon\| \quad (11)$$

Finally, using the result of lemma 2, it is straightforward to see that

$$-2\sqrt{\mu_{\boldsymbol{\theta}}} \leq \frac{\partial \mu_{\theta_i}}{\partial \theta_i} \leq 2\sqrt{\mu_{\boldsymbol{\theta}}} \quad (12)$$

□

We note that the partial derivative of the expectation value with respect to each parameter is a function of the expectation value itself. The elements of the random vector are sampled from a probability distribution bounded as per Eq. (12). As a result, in the case of minimisation problems, if the function value decreases in consecutive iterations, then the bounds on the gradients get tighter, and the approximation of the gradient with the random vector gets better. We ensure this through Lemma 4, where we find bounds on the step-size that guarantees a decrease in objective function value from one iteration to the next.

2.2 Quantum-Gradient Sampling Algorithm

In this section, we analyze the convergence of Algorithm 1. In Theorem 5, we observe that under Assumption 1, and with the correct choice of step-size α_t at each iteration, our algorithm achieves an asymptotic convergence rate of $O(1/\sqrt{T})$, which is equivalent to that of classical gradient descent, while requiring up to $\sim 2k$ fewer circuit-executions per iteration.

We begin by providing a bound on the step-size α_t that guarantees reduction in the objective function value.

Lemma 4. *At iteration t , there exists a step-size α_t which guarantees a decrease in the objective function value from $\mu^{(t)}$ to $\mu^{(t+1)}$ (as defined in Eq. (2)), corresponding to $\boldsymbol{\theta}^{(t)}$ and $\boldsymbol{\theta}^{(t+1)}$ (which are related as per Eq. (6)), where \mathbf{g}_s is a random vector $\in \mathbb{R}^k$.*

Proof. Let $\mathbf{H}(\boldsymbol{\zeta})$ denote the Hessian of $\mu_{\boldsymbol{\zeta}}$ (with $\boldsymbol{\zeta}$ being a convex combination of $\boldsymbol{\theta}^{(t)}$ and $\boldsymbol{\theta}^{(t+1)}$), and L its Lipschitz smoothness constant. From the Taylor expansion of $\mu^{(t+1)}$:

$$\begin{aligned} \mu^{(t+1)} - \mu^{(t)} &= s_t \alpha_t \mathbf{g}_t^\top \mathbf{g}_s + \frac{\alpha_t^2 s_t^2}{2} \mathbf{g}_s^\top \mathbf{H}(\boldsymbol{\zeta}) \mathbf{g}_s \\ &\leq -\alpha_t |\mathbf{g}_t^\top \mathbf{g}_s| + \frac{\alpha_t^2 L}{2} \|\mathbf{g}_s\|_2^2 \end{aligned} \quad (13)$$

Thus, we obtain the following range of α_t that guarantees reduction in function value:

$$0 \leq \alpha_t \leq \frac{2|\mathbf{g}_t^\top \mathbf{g}_s|}{L\|\mathbf{g}_s\|_2^2} \quad (14)$$

□

Theorem 5. *If the step-size α_t at each iteration satisfies Eq. (14), and the parameters θ are updated as per Eq. (6), then the Quantum-Gradient Sampling Algorithm converges in T iterations to a stationary point of μ_θ with a rate given by $O\left(\frac{1}{\sqrt{T}}\right)$.*

Proof. Choosing $\alpha_t = \frac{2|\mathbf{g}_t^\top \mathbf{g}_s|}{aL\|\mathbf{g}_s\|_2^2}$ with $a > 1$, Eq. (13) simplifies to:

$$\mu^{(t+1)} - \mu^{(t)} \leq -\frac{2}{aL} \left(1 - \frac{1}{a}\right) \|\mathbf{g}_t\|_2^2 \cos^2(\phi_t) \quad (15)$$

Taking expectation on both sides, and summing over t ,

$$\begin{aligned} \sum_{t=0}^{T-1} \mathbb{E} [\mu^{(t+1)} - \mu^{(t)}] &\leq -\frac{2}{aL} \left(1 - \frac{1}{a}\right) \sum_{t=0}^{T-1} \|\mathbf{g}_t\|_2^2 \mathbb{E} [\cos^2(\phi_t)] \\ \implies \mu^{(0)} - \mathbb{E}[\mu^{(T-1)}] &\geq \frac{2}{aL} \left(1 - \frac{1}{a}\right) T \epsilon_g^2 \mathbb{E} [\cos^2(\phi_t)] \\ \implies \mu^{(0)} - \mu^* &\geq \frac{2}{aL} \left(1 - \frac{1}{a}\right) T \epsilon_g^2 \mathbb{E} [\cos^2(\phi_t)] \end{aligned} \quad (16)$$

where ϕ_t is the angle between \mathbf{g}_s and \mathbf{g}_t at iteration t , and ϵ_g is a lower bound on the norm of the gradient of μ . \square

The choice of an appropriate step-size, as per Eq. (14), requires knowledge of the gradient at any given iteration. To circumvent this issue, we set the step-size to a sufficiently low value, and demonstrate empirically in Sec. 4.1 that this still leads to an advantage over gradient-based methods.

2.2.1 Requisite Number of Shots

The gradient-sampling method expends its two circuit evaluations in discerning the descent-direction at each iteration. We posit that this requires μ_{θ^+} and μ_{θ^-} to be evaluated with a lower precision, thus opening up the potential for using a lower number of shots, where $\theta^+ := \theta^{(t)} + \alpha_t \mathbf{g}_s$ and $\theta^- := \theta^{(t)} - \alpha_t \mathbf{g}_s$.

Proposition 6. *Evaluating μ (defined in Eq. (2)) with a precision of ϵ_μ and a confidence of $1 - \delta$ requires $n_\mu \geq \frac{1}{2\epsilon_\mu^2} \ln\left(\frac{2}{\delta}\right)$ shots.*

Proof. This follows directly from Hoeffding's inequality. \square

Proposition 7. *Finding if θ^+ (defined above) is a descent direction, i.e., $\mu_{\theta^+} \leq \mu^{(t)}$, with a confidence of $1 - \delta$ requires $n_g \geq \frac{1}{2(\mu^{(t)} - \mu_{\theta^+})^2} \ln\left(\frac{2}{\delta}\right)$ shots.*

Proof. Let $\hat{\mu}_{\theta^+}$ be an unbiased estimator of μ_{θ^+} . A simple geometrical analysis reveals that if $|\hat{\mu}_{\theta^+} - \mu_{\theta^+}| \geq |\mu^{(t)} - \mu_{\theta^+}|$, then we fail to correctly obtain the direction of descent. Using Hoeffding's inequality again to bound the probability of failure gives the necessary number of shots to be $n_g \geq \frac{1}{2(\mu^{(t)} - \mu_{\theta^+})^2} \ln\left(\frac{2}{\delta}\right)$. \square

Thus, when the difference in objective value between subsequent iterations is larger than ϵ_μ , gradient-sampling requires a lower number of shots than gradient-based methods. However, recent studies on stochastic gradient descent, and its variations, [9, 10, 11, 12] show that even using a very low number of shots (as few as a single shot) to estimate the gradient can result in adequate performance. Hence, it might be possible to incorporate the same shot-frugality into QGSA to obtain a reduction both in the number of circuit-executions and shots.

2.2.2 Termination Criteria

Though QGSA claims to use two circuit-evaluations per iteration, in practice, one iteration may suffice. One may choose to evaluate either μ_{θ^+} or μ_{θ^-} , and forgo the other if the corresponding θ^+ or θ^- is found to be a descent-direction, further reducing the number of circuits to be executed. In case neither of θ^+ or θ^- offers a reduction in the objective function value, the step-size may be diminished as $\alpha_{(t+1)} \leftarrow \alpha_t/(1+\gamma)$, where γ is a decay parameter ≥ 0 . If no reduction is obtained over a configurable number of iterations, for very low values of α_t , or for satisfactorily low bounds on the probability distribution, the algorithm may be terminated with the belief of having reached a (local) minimum.

2.2.3 Other Details

Finally, we hypothesize that QGSA may be more resilient to noise than the first-order methods that estimate the gradient, as the effects of noise may be absorbed within the stochasticity of the sampled parameters at each iteration. The proposed algorithm may also help navigate barren plateaus [17] due to its stochastic nature, as suggested in [12]. QGSA might also be combined with other first-order methods, natural gradient descent [18], and heuristics such as operator-grouping [19, 20, 21, 22, 23] (by replacing their gradient-estimation step), to enhance its performance.

3 Application to Binary Classification

Binary classification is one of the earliest use-cases to have been attempted using Quantum Machine Learning, and has been studied extensively [4, 5, 24, 25]. The motivation behind mentioning it here is to set up the context to describe the experiments, and results thereof, presented later in Sec. 4.1, and to introduce a new loss function to address binary classification. Without delving too much into the details, a binary classification model consists of a hypothesis function/model h_{θ} , which depends on trainable parameters θ . For each data point \mathbf{x}_i , the function returns a prediction, which is then compared against the available ground truth/label y_i through the use of a loss function \mathcal{L} . The overall empirical risk is defined as:

$$\hat{R}_h := \sum_{i=1}^n \mathcal{L}(h_{\theta}(\mathbf{x}_i), y_i) =: \mathcal{L}_{\theta} \quad (17)$$

A classical optimiser then adjusts the parameters to minimise the empirical risk to obtain a model that can be used to make predictions for unseen data points. It is important to mention that the hypothesis and loss functions make implicit assumptions and place a prior on the class-conditional density of the the data, and the promise of quantum computing in QML is to provide families of variational circuits/ansatzes that are classically difficult-to-simulate.

The QGSA, recalling from above, minimises functions of the form $\langle \psi(\theta) | H | \psi(\theta) \rangle$, where the eigenvalues of $H \in [0, 1]$. To provide a natural fit between this and the loss function, we define a new loss as:

$$\begin{aligned} \mathcal{L}_{QH}(h_{\theta}(\mathbf{x}), y) &:= \langle \psi(\theta, \mathbf{x}) | (I - y\mathcal{O}) | \psi(\theta, \mathbf{x}) \rangle \\ &= \frac{(1 - yh_{\theta}(\mathbf{x}))}{2} \end{aligned} \quad (18)$$

where $h_{\theta}(\mathbf{x}) = \langle \psi(\theta, \mathbf{x}) | \mathcal{O} | \psi(\theta, \mathbf{x}) \rangle$; \mathcal{O} is a user-defined, configurable observable whose eigenvalues lie between -1 and 1 ; and consequently, those of $(I - y\mathcal{O}) \in [0, 1]$ which

satisfies Assumption 1. The loss function proposed in Eq. (18) is very similar to the popularly used Hinge loss in classical ML, due to which we dub this as the Quantum Hinge (QH) loss. It must also be noted that restriction on eigenvalues of H is not a necessary condition for QGSA to work (as Theorem 5 is independent of this assumption), but is nevertheless a nice-to-have since it lets us appeal to Theorem 3 and obtain consistently-reducing bounds on the probability distribution. The QGSA algorithm, as such, works with arbitrary loss functions as exemplified in the subsequent section.

4 Experimental Details and Results

In this section, we provide details of the binary classification experiments that were conducted to investigate and compare the performance of QGSA against Gradient Descent (GD), Randomised Coordinate Descent (RCD), and SPSA, the former two of which use the PSR to estimate gradients, and the latter two use two function evaluations per iteration to update the parameters. The onus of this paper is not to propose good encoding schemes, ansätze or loss functions for the problem being considered, or even how the trained (ML) models generalise to unseen data points, but to compare the rate of decrease in objective function value with respect to the number of circuits executed.

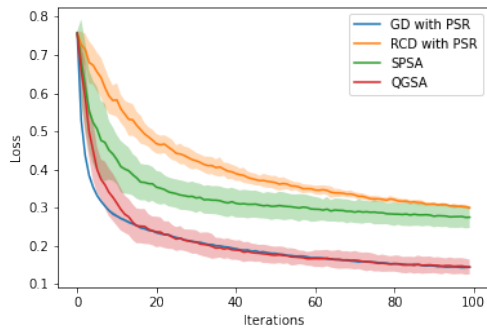
Binary classification was performed on the following two datasets:

- Iris dataset [26]: only the first two classes were considered and the features are translated and scaled to the range of $[0, \pi]$.
- Kaggle Surface Crack Detection dataset [27]: The entire dataset consists of 20,000 227×227 RGB examples each of images with and without cracks. 100 samples were randomly chosen from each class and preprocessed, as described in [28].

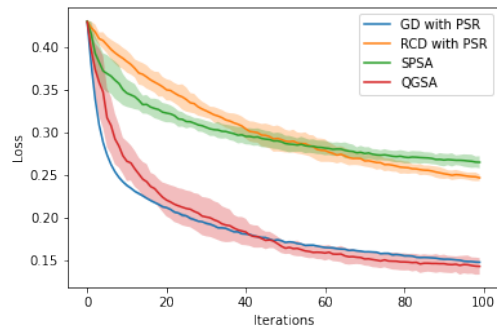
In both cases, the data points were labelled as $+1$ and -1 to denote the two classes. The classification circuits were created by first encoding the data into the qubits using the H gate, followed by the R_Z gate with the features passed as parameters to the latter. The encoding layer was followed up with 3 layers of the Basic Entangling Layers ansatz from PennyLane [29], numbering the optimisable parameters in the circuit at 12. Finally, $\langle Z \rangle$ of the first qubit in the circuit was measured, which played the role of $h_{\theta}(\mathbf{x})$. The models with both QH and Mean Squared Error (MSE) as the loss functions, using the four aforementioned methods. In each case, the models were initiated with the same starting point and trained for 100 iterations with step-size $\alpha = 0.1$ (in case of SPSA, the values of the hyperparameters were: $a = 0.1$, $\alpha = 0.602$, $c = 0.2$, and $\gamma = 0.101$, which were chosen as prescribed in [15], and a was chosen to make the comparison fair against QGSA, GD, and RCD) on the noise-free simulator available through PennyLane [29]. In case of gradient-sampling, both μ_{θ^+} and μ_{θ^-} were evaluated, and keeping the stochasticity of the processes in mind, we report the results over 10 trials.

4.1 Results and Observations

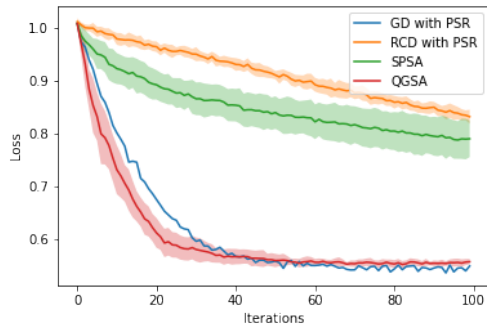
Fig. 1 depicts the plots of average training losses (over 10 experiments, along with their standard deviation) for binary classification of both the Iris and Crack datasets, using the classifiers detailed above. The training losses have been reported against the number of iterations of the optimisation procedure, as well as the total number of circuit executions used for updating the parameters. Both SPSA and RCD were found to require the same number of circuit evaluations on an average as GD, while QGSA consistently provided a dramatic reduction. To put this in perspective, training the classifier on the Crack dataset



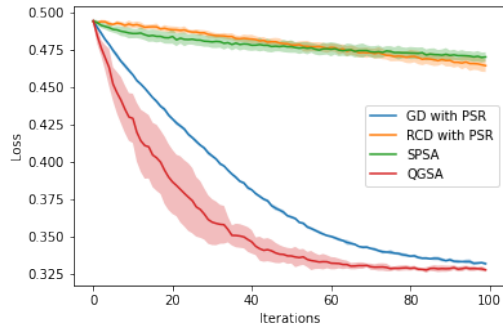
(a) Iris MSE



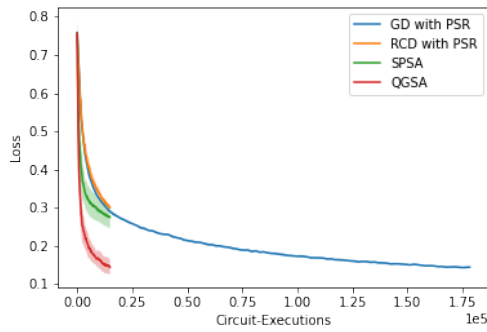
(b) Iris QH



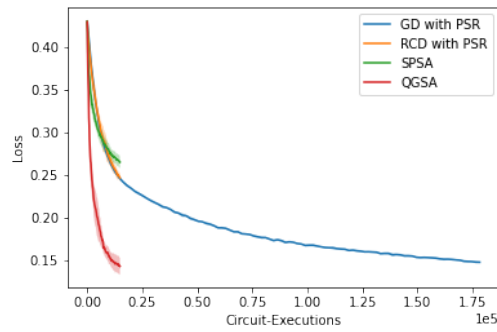
(c) Crack MSE



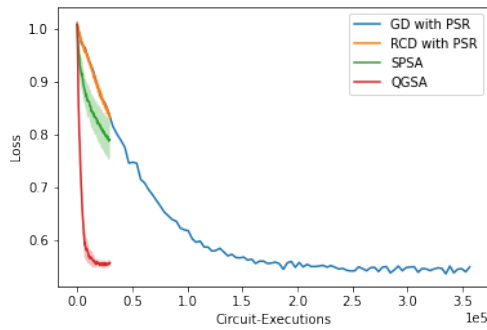
(d) Crack QH



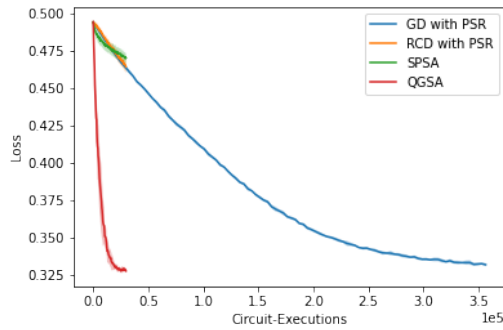
(e) Iris MSE



(f) Iris QH



(g) Crack MSE



(h) Crack QH

Figure 1: Plots of training losses on the y-axis against the number of iterations or the number of circuit-executions expended on updating the parameters on the x-axis, for both the Iris and Crack datasets. Sec. 4 provides details on the classifier used, and the caption of each individual subfigure identifies the data set and the loss function.

with QH loss using GD on a superconducting qubit based processor available through the aforementioned cloud service provider would consume \sim USD 230,000. In comparison, using QGSA, the same activity would require only about USD 18,000. Further, it may be observed that QGSA uses approximately the same number of iterations as GD, both of which perform a lot better than RCD and SPSA.

5 Conclusion and Future Directions

In this paper, we presented Quantum-Gradient Sampling Algorithm which uses random vectors drawn from bounded probability distributions, instead of estimating gradients, to update the parameters in variational quantum circuits. We also proved that QGSA has the same asymptotic rate of convergence as gradient descent, and demonstrated its capability through binary classification on two different datasets. The results showed a k -fold reduction in the number of circuit executions on an average through the use of QGSA. The development of QGSA may be carried forward by incorporating it into first-order methods as a substitute for the gradient estimation step, and further reducing the requisite number of shots through shot-frugal methods. The performance of QGSA may also be investigated in navigating barren plateaus and providing resilience against noise.

References

- [1] John Preskill. Quantum computing in the NISQ era and beyond. *Quantum*, 2:79, aug 2018.
- [2] Alberto Peruzzo, Jarrod McClean, Peter Shadbolt, Man-Hong Yung, Xiao-Qi Zhou, Peter J. Love, Alán Aspuru-Guzik, and Jeremy L. O’Brien. A variational eigenvalue solver on a photonic quantum processor. *Nature Communications*, 5(1), jul 2014.
- [3] Edward Farhi, Jeffrey Goldstone, and Sam Gutmann. A quantum approximate optimization algorithm, 2014.
- [4] Maria Schuld, Alex Bocharov, Krysta M. Svore, and Nathan Wiebe. Circuit-centric quantum classifiers. *Physical Review A*, 101(3), mar 2020.
- [5] Andrea Mari, Thomas R. Bromley, Josh Izaac, Maria Schuld, and Nathan Killoran. Transfer learning in hybrid classical-quantum neural networks. *Quantum*, 4:340, oct 2020.
- [6] Abhinav Kandala, Antonio Mezzacapo, Kristan Temme, Maika Takita, Markus Brink, Jerry M. Chow, and Jay M. Gambetta. Hardware-efficient variational quantum eigensolver for small molecules and quantum magnets. *Nature*, 549(7671):242–246, sep 2017.
- [7] Maria Schuld, Ville Bergholm, Christian Gogolin, Josh Izaac, and Nathan Killoran. Evaluating analytic gradients on quantum hardware. *Physical Review A*, 99(3), mar 2019.
- [8] K. Mitarai, M. Negoro, M. Kitagawa, and K. Fujii. Quantum circuit learning. *Physical Review A*, 98(3), sep 2018.
- [9] Jonas M. Kübler, Andrew Arrasmith, Lukasz Cincio, and Patrick J. Coles. An adaptive optimizer for measurement-frugal variational algorithms. *Quantum*, 4:263, may 2020.
- [10] Andrew Arrasmith, Lukasz Cincio, Rolando D. Somma, and Patrick J. Coles. Operator sampling for shot-frugal optimization in variational algorithms, 2020.

- [11] Ryan Sweke, Frederik Wilde, Johannes Meyer, Maria Schuld, Paul K. Faehrmann, Barthé lémy Meynard-Piganeau, and Jens Eisert. Stochastic gradient descent for hybrid quantum-classical optimization. *Quantum*, 4:314, aug 2020.
- [12] Shiro Tamiya and Hayata Yamasaki. Stochastic gradient line bayesian optimization for efficient noise-robust optimization of parameterized quantum circuits. *npj Quantum Information*, 8(1), jul 2022.
- [13] Vyacheslav Kungurtsev, Georgios Korpas, Jakub Marecek, and Elton Yechao Zhu. Iteration complexity of variational quantum algorithms, 2022.
- [14] James C. Spall. An overview of the simultaneous perturbation method for efficient optimization. *Johns Hopkins Apl Technical Digest*, 19:482–492, 1998.
- [15] J.C. Spall. Implementation of the simultaneous perturbation algorithm for stochastic optimization. *IEEE Transactions on Aerospace and Electronic Systems*, 34(3):817–823, 1998.
- [16] Lecture notes on randomised coordinate descent. <https://www.cs.ubc.ca/~schmidtm/Courses/540-W19/L10.pdf#page5>. Accessed: 2023-06-20.
- [17] Jarrod R. McClean, Sergio Boixo, Vadim N. Smelyanskiy, Ryan Babbush, and Hartmut Neven. Barren plateaus in quantum neural network training landscapes. *Nature Communications*, 9(1), nov 2018.
- [18] James Stokes, Josh Izaac, Nathan Killoran, and Giuseppe Carleo. Quantum natural gradient. *Quantum*, 4:269, may 2020.
- [19] Andrew Jena, Scott Genin, and Michele Mosca. Pauli partitioning with respect to gate sets, 2019.
- [20] Artur F. Izmaylov, Tzu-Ching Yen, Robert A. Lang, and Vladyslav Verteletskyi. Unitary partitioning approach to the measurement problem in the variational quantum eigensolver method, 2019.
- [21] Tzu-Ching Yen, Vladyslav Verteletskyi, and Artur F. Izmaylov. Measuring all compatible operators in one series of a single-qubit measurements using unitary transformations, 2020.
- [22] Pranav Gokhale, Olivia Angiuli, Yongshan Ding, Kaiwen Gui, Teague Tomesh, Martin Suchara, Margaret Martonosi, and Frederic T. Chong. Minimizing state preparations in variational quantum eigensolver by partitioning into commuting families, 2019.
- [23] Ophelia Crawford, Barnaby van Straaten, Daochen Wang, Thomas Parks, Earl Campbell, and Stephen Brierley. Efficient quantum measurement of pauli operators in the presence of finite sampling error. *Quantum*, 5:385, jan 2021.
- [24] Maria Schuld. Supervised quantum machine learning models are kernel methods, 2021.
- [25] Vojtěch Havlíček, Antonio D. Córcoles, Kristan Temme, Aram W. Harrow, Abhinav Kandala, Jerry M. Chow, and Jay M. Gambetta. Supervised learning with quantum-enhanced feature spaces. *Nature*, 567(7747):209–212, mar 2019.
- [26] R. A. Fisher. Iris. UCI Machine Learning Repository, 1988. DOI: <https://doi.org/10.24432/C56C76>.
- [27] Surface crack detection dataset. <https://www.kaggle.com/datasets/arunrk7/surface-crack-detection>. Accessed: 2023-06-20.

- [28] Sayantan Pramanik, M Girish Chandra, C V Sridhar, Aniket Kulkarni, Prabin Sahoo, Chethan D V Vishwa, Hrishikesh Sharma, Vidyut Navelkar, Sudhakara Poojary, Pranav Shah, and Manoj Nambiar. A quantum-classical hybrid method for image classification and segmentation. In *2022 IEEE/ACM 7th Symposium on Edge Computing (SEC)*, pages 450–455, 2022.
- [29] Ville Bergholm, et al. Pennylane: Automatic differentiation of hybrid quantum-classical computations, 2022.

A Practical QGSA

Algorithm 2 Practically implementable Quantum-Gradient Sampling Algorithm

Inputs: Step-size α , step-size decay parameter γ , initial point $\boldsymbol{\theta}^{(0)}$, n_μ , n_g , number of iterations T , $t = 0$

start

$\boldsymbol{\theta} \leftarrow \boldsymbol{\theta}^{(0)}$

for $t \in [T]$ **do**

 evaluate $\mu^{(t)}$ with n_μ shots

$\mathbf{g}_s \sim \mathbb{P} \left(-2\sqrt{\mu^{(t)}}, 2\sqrt{\mu^{(t)}} \right)$

 ▷ where \mathbb{P} is a probability density function bounded

 between $-2\sqrt{\mu^{(t)}}$ and $2\sqrt{\mu^{(t)}}$

$\boldsymbol{\theta}^- \leftarrow \boldsymbol{\theta} - \alpha \mathbf{g}_s$

 evaluate $\mu_{\boldsymbol{\theta}^-}$ with n_g shots

if $\mu_{\boldsymbol{\theta}^-} < \mu^{(t)}$ **then**

$\boldsymbol{\theta} \leftarrow \boldsymbol{\theta}^-$

else

$\boldsymbol{\theta}^+ \leftarrow \boldsymbol{\theta} + \alpha \mathbf{g}_s$

 evaluate $\mu_{\boldsymbol{\theta}^+}$ with n_g shots

if $\mu_{\boldsymbol{\theta}^+} < \mu^{(t)}$ **then**

$\boldsymbol{\theta} \leftarrow \boldsymbol{\theta}^+$

else

$\alpha \leftarrow \frac{\alpha}{1+\gamma}$

end if

end if

end for

return $\boldsymbol{\theta}$

end
